Astron. Astrophys. 317, 610–617 (1997)

ASTRONOMY
AND
ASTROPHYSICS

Dynamos with different formulations of a dynamic α–effect

Eurico Covas[1,*], **Andrew Tworkowski**[1,**], **Axel Brandenburg**[2,***], **and Reza Tavakol**[1,†]

[1] Astronomy Unit, School of Mathematical Sciences, Queen Mary and Westfield College, Mile End Road, London E1 4NS, UK
[2] Department of Mathematics and Statistics, University of Newcastle upon Tyne NE1 7RU, UK

Received 26 April 1996 / Accepted 4 June 1996

Abstract. We investigate the behaviour of $\alpha\Omega$ dynamos with a dynamic α, whose evolution is governed by the imbalance between a driving and a damping term. We focus on truncated versions of such dynamo models which are often studied in connection with solar and stellar variability. Given the approximate nature of such models, it is important to study how robust they are with respect to reasonable changes in the formulation of the driving and damping terms. For each case, we also study the effects of changes of the dynamo number and its sign, the truncation order and initial conditions. Our results show that changes in the formulation of the driving term have important consequences for the dynamical behaviour of such systems, with the detailed nature of these effects depending crucially on the form of the driving term assumed, the value and the sign of the dynamo number and the initial conditions. On the other hand, the change in the damping term considered here seems to produce little qualitative effect.

Key words: Sun: magnetic fields – stars: magnetic fields – MHD – chaos

1. Introduction

It is commonly believed that the observed solar and stellar variabilities have their origin in the hydromagnetic dynamos associated with turbulent convection zones. Numerical studies have been made using the full magneto-hydrodynamical partial differential equations (PDE), which reproduce some features of solar and stellar dynamos (e.g. Gilman 1983). Such models are fairly complex and do not allow extensive parameter surveys. As a result, a number of alternatives to the direct integration of PDE have been pursued. Among these has been the employment of the mean field dynamo formalism (Krause & Rädler 1980) in order to construct various types of dynamos, such as $\alpha\Omega$ dynamo models. Despite the fact that such models have been shown to be capable of producing a large number of observationally relevant modes of behaviour, ranging from stationary to chaotic (cf. Brandenburg et al. 1989a,b; Tavakol et al. 1995), they nevertheless involve a number of unknown features such as the exact nature of the nonlinearities involved. Furthermore, in order to clarify the origin of dynamical modes of behaviour observed in dynamo models, further simplifications of these models have been considered, involving low dimensional truncations of the governing PDE. Such models have also been shown to be capable of producing a number of important features of stellar variability including periodic, intermittent and chaotic modes of behaviour (Zeldovich et al. 1983; Weiss et al. 1984; Feudel et al. 1993).

Now given that these models are cheaper to integrate and more transparent to study, it would be very useful if we could employ them as diagnostic tools in order to study the effects of introducing different parametrisations and nonlinearities involved. The problem, however, is that these low dimensional models involve severe approximations, and therefore in order to be able to take the results produced by them as physically relevant, it is important that they remain robust under changes which fall within the domain of the approximations assumed. This is particularly of importance since on the basis of results from dynamical systems theory, structurally stable systems are not everywhere dense in the space of dynamical systems (Smale 1966), in the sense that small changes in models can produce qualitatively important changes in their dynamics. In this way the appropriate theoretical framework for the construction of mathematical models and the analysis of observational data may turn out to be that of structural fragility (Tavakol & Ellis 1988; Coley & Tavakol 1992; Tavakol et al. 1995).

Here as examples of such changes we shall consider first changes in the order of truncation and then changes in the details of the physics assumed. Regarding the former, a number of attempts have already been made to study the effects of increasing the truncation order on the resulting dynamics. For example, Schmalz & Stix (1991) (hereafter referred to as S&S91) have looked at the detailed dynamics of the low dimensional truncations of the mean field dynamo equations and have studied

Send offprint requests to: Eurico Covas
* e-mail: E.O.Covas@qmw.ac.uk
** e-mail: A.S.Tworkowski@qmw.ac.uk
*** e-mail: Axel.Brandenburg@ncl.ac.uk
† e-mail: reza@maths.qmw.ac.uk

what happens as the order of the truncation is increased, while Tobias et al. (1995) have employed normal form theory to construct a robust minimal third order model which exhibits both the modulation of basic cycles and chaos. These studies have shown that low dimensional models can capture a number of important dynamical features of the dynamo models.

Our aim in this paper is complementary to that of the above authors. We take a detailed look at the results in S&S91 and ask to what extent these results remain robust as reasonable changes are made to the details of the physics employed, and in each case we study how such changes affect the dynamical behaviour of different truncations.

2. Models with dynamical α

The starting point of the truncated dynamical α models considered in S&S91 is the mean field induction equation

$$\frac{\partial \boldsymbol{B}}{\partial t} = \nabla \times (\boldsymbol{v} \times \boldsymbol{B} + \alpha \boldsymbol{B} - \eta_t \nabla \times \boldsymbol{B}), \tag{1}$$

where $\boldsymbol{B}$ and $\boldsymbol{v}$ are the mean magnetic field and the mean velocity, respectively. The turbulent magnetic diffusivity η_t and the coefficient α, which relates the mean electrical current arising in helical turbulence (the α–effect) to the mean magnetic field, both arise from the correlation of small scale (turbulent) velocity and magnetic fields (Krause & Rädler 1980).

S&S91 employ an axisymmetrical configuration with one spatial dimension x, which corresponds to a latitude coordinate and a longitudinal velocity with a constant radial gradient (the vertical shear ω_0). The magnetic field takes the form

$$\boldsymbol{B} = \left(0, B_\phi, \frac{1}{R}\frac{\partial A_\phi}{\partial x}\right), \tag{2}$$

where A_ϕ is the ϕ–component (latitudinal) of the magnetic vector potential, B_ϕ the ϕ–component of $\boldsymbol{B}$ and x is measured in terms of the stellar radius R. These assumptions allow Eq. (1) to be split into

$$\frac{\partial A_\phi}{\partial t} = \frac{\eta_t}{R^2}\frac{\partial^2 A_\phi}{\partial x^2} + \alpha B_\phi, \tag{3}$$

$$\frac{\partial B_\phi}{\partial t} = \frac{\eta_t}{R^2}\frac{\partial^2 B_\phi}{\partial x^2} + \frac{\omega_0}{R}\frac{\partial A_\phi}{\partial x}. \tag{4}$$

In S&S91, α is divided into a static (kinematic) and a dynamic (magnetic) part: $\alpha = \alpha_0 \cos x - \alpha_M(t)$, with its time-dependent part $\alpha_M(t)$ satisfying an evolution equation in the form

$$\frac{\partial \alpha_M}{\partial t} = \Delta(\alpha_M) + f(\boldsymbol{B}), \tag{5}$$

where Δ is a damping operator and $f(\boldsymbol{B})$ is a pseudo-scalar that is quadratic in the magnetic filed.

It has been argued that the α effect is quenched by the current helicity density $\boldsymbol{J}\cdot\boldsymbol{B}$, which in turn is governed by a dynamical equation (Kleeorin & Ruzmaikin 1982; Zeldovich et al. 1983). The reason the feedback (quenching) is not instantaneous is a consequence of the fact that the magnetic helicity is conserved in the absence of diffusion or boundary effects. Such models have been investigated recently by Kleeorin et al. (1995). In S&S91 a truncated version of yet another model was studied, in which instead of the current helicity density, the magnetic helicity density $\boldsymbol{A}\cdot\boldsymbol{B}$, or rather $A_\phi B_\phi$, was used. Their model was motivated on heuristic grounds. Bifurcation properties of a truncated version of a similar model, but with a different damping term, have been studied by Feudel et al. (1993). Our present investigation is thus motivated partially by the variety of models presented in the literature. It is important to know what is the effect of the dynamical feedback and how the different representations affect the results.

To proceed S&S91 specify the feedback in the following way

$$f(\boldsymbol{B}) \propto A_\phi B_\phi \tag{6}$$

and then look at various $N-$modal truncations of these equations and study what happens to the dynamical behaviour of the resulting systems as N is increased.

To do this it is convenient to transform these equations into a non-dimensional form. This can be done by employing a reference field B_0, measuring time in units of R^2/η_t and defining the following non-dimensional quantities

$$A = \frac{R\omega_0}{B_0\eta_t}A_\phi, \quad B = \frac{B_\phi}{B_0}, \quad C = \frac{\alpha_M R^3\omega_0}{\eta_t^2}, \tag{7}$$
$$\nu = \frac{\nu_t}{\eta_t}, \quad D = \frac{\alpha_0\omega_0 R^3}{\eta_t^2},$$

where ν_t is the turbulent diffusivity. Eqs. (3), (4) and (5) with the damping operator taken to be

$$\Delta = \frac{\nu_t}{R^2}\frac{\partial^2}{\partial x^2}, \tag{8}$$

can then be rewritten in the following non-dimensional forms:

$$\frac{\partial A}{\partial t} = \frac{\partial^2 A}{\partial x^2} + DB\cos x - CB, \tag{9}$$

$$\frac{\partial B}{\partial t} = \frac{\partial^2 B}{\partial x^2} + \frac{\partial A}{\partial x}, \tag{10}$$

$$\frac{\partial C}{\partial t} = \nu\frac{\partial^2 C}{\partial x^2} + AB. \tag{11}$$

Now considering the interval $0 \le x \le \pi$ (which corresponds to the full range of latitudes), taking the boundary conditions at $x = 0$ and $x = \pi$ to be given by $A = B = C = 0$ and using a spectral expansion of the form

$$A = \sum_{n=1}^{N} A_n(t)\sin nx, \tag{12}$$

$$B = \sum_{n=1}^{N} B_n(t)\sin nx, \tag{13}$$

$$C = \sum_{n=1}^{N} C_n(t)\sin nx, \tag{14}$$

allows the set of Eqs. (9–11) to be transformed into the form

$$\frac{\partial A_n}{\partial t} = -n^2 A_n + \frac{D}{2}(B_{n-1} + B_{n+1}) + \sum_{m=1}^{N}\sum_{l=1}^{N} F(n,m,l) B_m C_l, \tag{15}$$

$$\frac{\partial B_n}{\partial t} = -n^2 B_n + \sum_{m=1}^{N} G(n,m) A_m, \tag{16}$$

$$\frac{\partial C_n}{\partial t} = -\nu n^2 C_n - \sum_{m=1}^{N}\sum_{l=1}^{N} F(n,m,l) A_m B_l, \tag{17}$$

where

$$F(n,m,l) = \frac{8nml}{\pi(n+m+l)(n+m-l)(n-m+l)(n-m-l)}, \tag{18}$$

if $n+m+l$ is odd and $F(n,m,l) = 0$ otherwise and

$$G(n,m) = \frac{4nm}{\pi(n^2-m^2)}, \tag{19}$$

if $n+m$ is odd and $G(n,m) = 0$ otherwise.

These rules enable the system to describe fields which are strictly symmetric (i.e. having only components B_n with odd n and A_n and C_n with even n) or strictly antisymmetric (i.e. having only components A_n with odd n and B_n and C_n with even n) with respect to $x = \pi/2$, provided the initial conditions have either of these parities.

Using these equations, S&S91 studied a number of such truncations numerically by varying the dynamo number D at each truncation N. Their main conclusions were:

1. With the choice of the driving term f given by Eq. (6) the antisymmetric truncation with the smallest non-trivial indices is identical with the Lorenz system (Lorenz 1963).
2. Different truncations are capable of producing stationary, oscillatory and chaotic modes of behaviour. They also make observations about the changes in the route to chaos, and conclude that, as N is increased, the route changes from period doubling to the Ruelle–Takens–Newhouse scenario (Ruelle & Takens 1971; Newhouse et al. 1978).
3. The qualitative behaviour of the truncations stabilises as the number of modes is increased and in particular for $N > 6$. As an example they observe that as N is increased the limit cycles remain stable for larger dynamo numbers.
4. They also discuss very briefly the $D < 0$ case, observing that the $N = 2$ case is always a stable fixed point and that for $N \geq 6$ the antisymmetric limit cycle becomes unstable via a saddle node bifurcation[1].

Now, as mentioned above, there are arguments in support of both the form of the driving term as well as the damping term being different (Kleeorin et al. 1995). So as a first step, we shall study, in the next section, how robust the results in S&S91 are with respect to various physically justified changes in the driving term that have been considered in the literature in Eq. (5). In Sect. 4 we study the effects of changes in the damping term.

[1] Care must be taken when speaking of antisymmetric solutions. In our studies we mean strictly antisymmetric solutions, while in S&S91 these also refers to the antisymmetric part of mixed parity solutions.

3. Robustness with respect to changes in the driving term

The general physically motivated choice for the driving term is given by Kleeorin & Ruzmaikin (1982), Zeldovich et al. (1983) and Kleeorin et al. (1995) to be in the form

$$f = W_1 \boldsymbol{J} \cdot \boldsymbol{B} + W_2 \alpha |\boldsymbol{B}|^2, \tag{20}$$

where W_1 and W_2 are constants. To study the effects of each term separately, we shall proceed by considering the cases $W_1 \neq 0$ ($W_2 = 0$) and $W_1 \neq 0$ ($W_2 \neq 0$) in the following sections.

3.1. Case (I): $f = W_1 \boldsymbol{J} \cdot \boldsymbol{B} + W_2 \alpha |\boldsymbol{B}|^2$, with $W_1 \neq 0$ ($W_2 = 0$)

Taking f to be of the form $f \propto \boldsymbol{J} \cdot \boldsymbol{B}$, substituting for $\boldsymbol{B}$ from Eq. (2) and recalling that $\boldsymbol{J} = \nabla \times \boldsymbol{B}$ we obtain

$$\boldsymbol{J} \cdot \boldsymbol{B} = (\nabla \times \boldsymbol{B}) \cdot \boldsymbol{B} = \frac{B_0^2 \eta_t}{R^3 \omega_0} \left(\frac{\partial A}{\partial x}\frac{\partial B}{\partial x} - \frac{\partial^2 A}{\partial x^2} B \right), \tag{21}$$

which allows Eq. (11) to be written as

$$\frac{\partial C}{\partial t} = \nu \frac{\partial^2 C}{\partial x^2} + \frac{\partial A}{\partial x}\frac{\partial B}{\partial x} - \frac{\partial^2 A}{\partial x^2} B. \tag{22}$$

Proceeding in a similar way as in previous section we obtain an identical set of differential equations to those obtained in S&S91, except that Eq. (17) is now changed to

$$\frac{\partial C_n}{\partial t} = -\nu n^2 C_n - \sum_{m=1}^{N}\sum_{l=1}^{N} H(n,m,l) A_m B_l, \tag{23}$$

where

$$H(n,m,l) = \frac{4}{\pi}\frac{nml(-n^2+3m^2+l^2)}{(n+l+m)(n+l-m)(n-l+m)(n-l-m)}, \tag{24}$$

if $n+m+l$ is odd and $H(n,m,l) = 0$ otherwise. The function H is clearly different from F unless $F = 0$, in which case H is also equal to zero.

For this system we can study also the pure antisymmetric and symmetric solutions, but for the sake of comparison with the results in S&S91 we confined ourselves to the antisymmetric solutions.

Now for the case of $N = 2$, the Eqs. (15), (16) and (23) become

$$\frac{dA_1}{dt} = -A_1 + \frac{DB_2}{2} - \frac{32 B_2 C_2}{15\pi}, \tag{25}$$

$$\frac{dB_2}{dt} = -4B_2 + \frac{8A_1}{3\pi}, \tag{26}$$

$$\frac{dC_2}{dt} = -4\nu C_2 + \frac{16 A_1 B_2}{5\pi}, \tag{27}$$

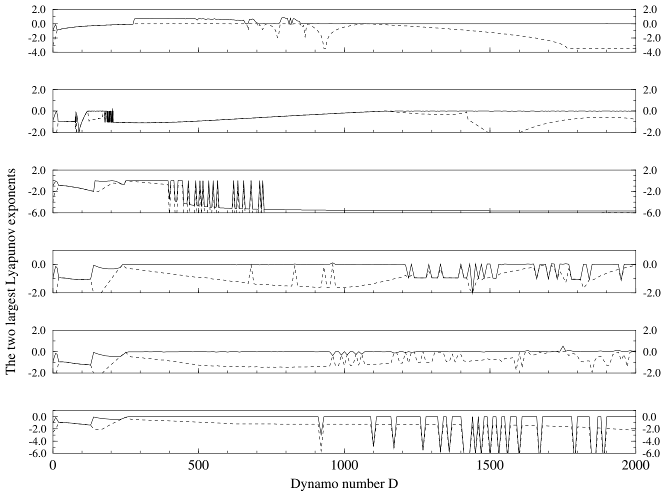

Fig. 1. Graphs of the two largest Lyapunov exponents for $N = 2, 4, 6, 7, 8$ and 10 (increasing downwards) for the case where $f \propto \boldsymbol{J} \cdot \boldsymbol{B}$ and $D > 0$

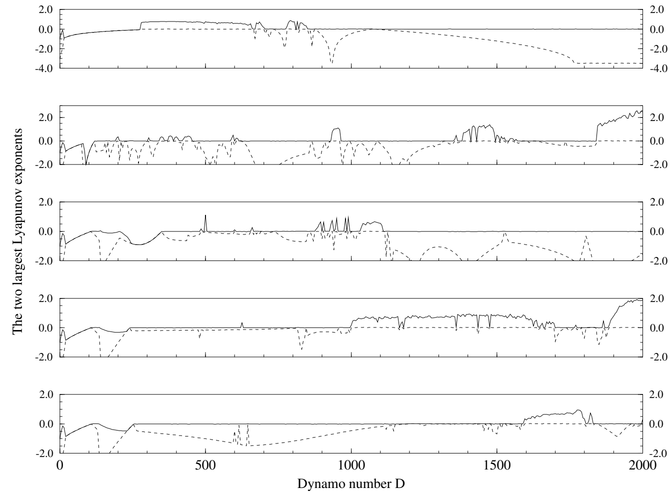

Fig. 2. Graphs of the two largest Lyapunov exponents for $N = 2, 4, 6, 7$, and 8 (increasing downwards) for the case where $f \propto A_\phi B_\phi$ and $D > 0$

which upon using the transformations

$$A_1 = \frac{15\sqrt{6}\pi^2}{64}Y, \quad B_2 = \frac{5\sqrt{6}\pi}{32}X, \quad C_2 = \frac{45\,\pi^2}{64}Z, \qquad (28)$$

result, as in S&S91, in the usual Lorenz equations (Lorenz 1963), with the control parameters given by $\sigma = 4$, $b = 4\nu$, and $r = D/3\pi$. To be compatible with S&S91 we also used $\nu = 0.5$ throughout[2].

Since our aim is to study the qualitative effects brought about by the changes in the form of f, we will not delve deeply into the details of the dynamics, such as the routes to chaos, and concentrate instead on the occurrence of equilibrium, periodic (including quasiperiodic) and chaotic regimes. Accordingly, the tools we employ are the time series and the spectra of Lyapunov exponents. The latter is particularly useful as a relatively sensitive tool to characterise the dynamics, with the Lyapunov spectra of the types $(-, -, -, \ldots)$, $(0, -, -, \ldots)$, $(0, 0, -, \ldots)$ and $(+, 0, -, \ldots)$ corresponding to equilibrium, periodic, quasiperiodic (with two periods) and chaotic regimes respectively. Also to keep the numerical costs reasonable, the resolution of D in all the figures was, unless stated otherwise, taken to be $D = 5$.

Now given the fact that in many astrophysical settings (including that of the sun) the sign of the dynamo number is not known, we shall also study the effects of changes in the sign of D.

We note also that the $\alpha\Omega$ dynamo concept becomes invalid if D exceeds a certain limit (Choudhuri 1990). Furthermore, in general, as D is increased more modes (higher N) are required to achieve convergence (numerically bounded solutions).

[2] These authors seem to confine themselves to this value of ν in order to obtain chaotic behaviour, for which one requires $\sigma > b + 1$ (Sparrow 1982). This amounts to the expectation that α relaxes much more slowly than the magnetic field.

3.1.1. Results for positive dynamo numbers

For the sake of comparison with S&S91, we studied the dynamics of the system (15, 16, 23), for different values of the truncation order N. A summary of our numerical results is given in Fig. 1 which is a plot of the two largest Lyapunov exponents as a function of the dynamo number for different truncations. In the following figures, the largest Lyapunov exponent is depicted by a solid line and its negative, zero and positive values indicate equilibrium, periodic and chaotic regimes. The simultaneous vanishing of the second Lyapunov exponent would imply the presence of quasiperiodic motion with two frequencies (i.e. motion on a 2–torus). It was not necessary to plot the third exponent, since no motion on T^3 or higher dimensional tori was observed which is not surprising in view of the results of Newhouse et al. (1978).

For a more transparent comparison, we have also produced in Fig. 2 an analogous figure for the system considered in S&S91. As the comparison of the Figs. 1 and 2 shows, the main differences produced by the replacement of $A_\phi B_\phi$ by $\boldsymbol{J} \cdot \boldsymbol{B}$ are as follows:

1. The chaotic regimes become less likely in the $\boldsymbol{J} \cdot \boldsymbol{B}$ case, in the sense that the intervals of the dynamo number D over which the system is chaotic decrease dramatically.
2. There exist indications for the presence of "multiple attractors" over substantial intervals of D, consisting of equilibrium and periodic states. These can be seen as regions of spiky behaviour in the solid line in Fig. 1, for certain truncations ($N = 4, 6, 7, 8, 10$). The behaviour of the system alternates between fixed point solutions (where all exponents are negative) and periodic orbits (where only the first one is zero) as the dynamo number D is slightly changed.
   The presence of such behaviour is potentially of great interest since it suggests that there exist intervals of D in which small changes in D can drastically change the behaviour of

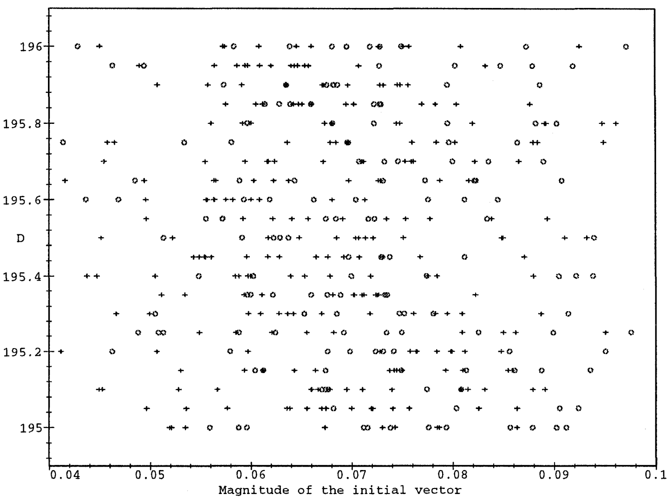

Fig. 3. Fragility in the dynamics with respect to small changes in the dynamo number D and the magnitude of the initial vector (A_n, B_n, C_n). A cross represents a fixed point while a circle represents a limit cycle. The initial conditions correspond to randomly chosen vectors of specified magnitude

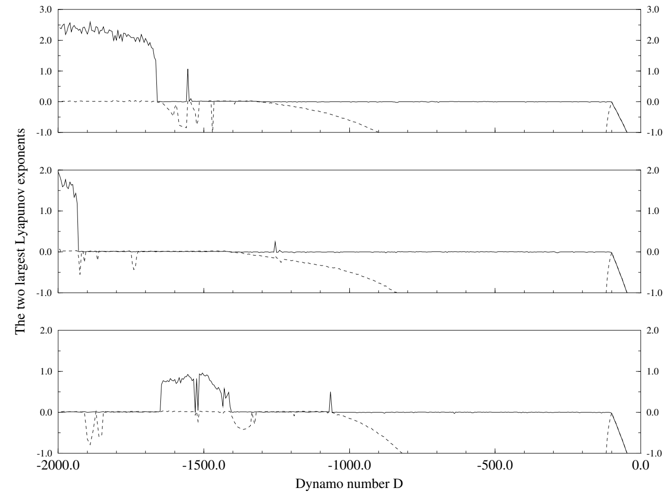

Fig. 4. Graphs of the two largest Lyapunov exponents for N = 7, 8, and 10 (increasing downwards) for the case when $f \propto \boldsymbol{J} \cdot \boldsymbol{B}$ and $D < 0$

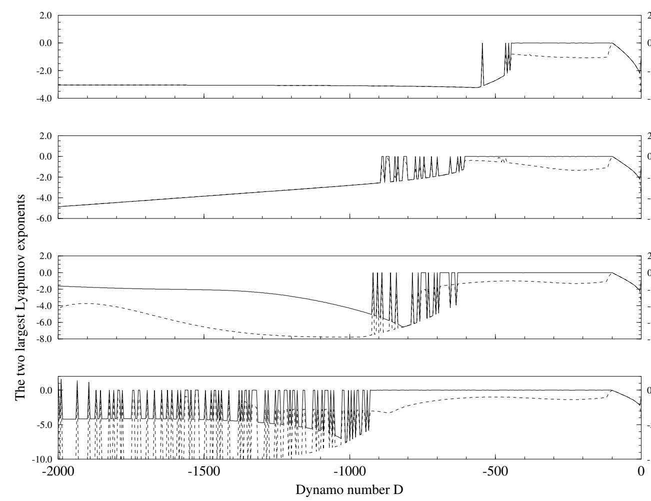

Fig. 5. Graphs of the two largest Lyapunov exponents for N = 4, 6, 7, and 8 (increasing downwards) for the case when $f \propto A_\phi B_\phi$ and $D < 0$

the system. This is also interesting, if one considers settings in which D or the initial conditions (IC) can vary slightly, but randomly, as the resulting behaviour would look very much like intermittency. To highlight this we have plotted in Fig. 3 the behaviour of the N = 4 truncation as a function of small changes in the dynamo number and the IC. As can be seen, small changes in either D or IC can produce important changes in the behaviour of the system. This therefore shows that there are substantial regions of D over which the behaviour of the system is sensitive to small changes in D and IC. Further, we have checked that this fragility is itself robust in the sense that taking a finer mesh of D does not qualitatively change this overall behaviour.

3. Regarding the overall behaviour of the systems with respect to increases in N, we observe the following. For small dynamo numbers, the behaviour seems to settle down to equilibrium and periodic states as N is increased. For example as can be seen from Fig. 1, for dynamo numbers up to $D \approx 900$, the behaviour settles down for $N \geq 7$. For larger values of D, however, we observe an increase in the dominance of the "multiple attractor" regime for the values of N considered here. It is likely, however, that with increasing N, these intervals only establish themselves at higher values of D.
4. The transition to chaos appears to be very abrupt in the N = 2 case, with the system going from a fixed point into a chaotic regime very rapidly, at least to within a resolution of $\Delta D \approx 10^{-4}$, with no intermediate behaviour being observed. For the case N = 3 the system goes from a fixed point $\rightarrow$ limit cycle $\rightarrow$ chaos. For still higher N, our calculations indicate that chaos becomes scarce.
5. Chaotic regions were also found in the "multiple attractors" region, which were fragile with respect to small changes in the IC and the choice of D.

3.1.2. Results for negative dynamo numbers

Our results for the negative dynamo numbers are shown in Fig. 4. Also, in view of the sparseness of the results reported in S&S91 for the models with negative dynamo numbers, we present Fig. 5 as an analogous figure for their case.

The main features of these models are:

1. The chaotic regimes seem to become less likely in the $A_\phi B_\phi$ case. In fact, for the mesh size in D taken here, we only observed chaotic solutions in the case of N = 8 and then only for very high dynamo numbers.
2. There are substantial intervals (in D) of "multiple attractors" (consisting of equilibrium and periodic states) for the $A_\phi B_\phi$ case.
3. In both cases the behaviour for $D \gtrsim -900$ stabilises as N is increased. This occurs for $N \geq 2$ for the equilibrium

regime and $N \geq 7$ for periodic regime. These results also indicate that there are parallels between the $A_\phi B_\phi$ case with negative dynamo numbers and the $\boldsymbol{J}\cdot\boldsymbol{B}$ case with positive dynamo numbers. In both cases, multiple attractor regions seem to dominate for large D values, as N is increased.

4. For high $N(\geq 7)$ in the $\boldsymbol{J}\cdot\boldsymbol{B}$ case, the transition is from T^2 to chaotic behaviour. This does not seem not true for $N = 4, 5, 6$ where the chaotic behaviour seems to appear abruptly.

3.2. *Case (II): $f = W_1\boldsymbol{J}\cdot\boldsymbol{B} + W_2\alpha|\boldsymbol{B}|^2$, with $W_1 \neq 0$ and $W_2 \neq 0$*

To study the effects of including the $\alpha|\boldsymbol{B}|^2$ term, we use the dynamic α equation from Kleeorin & Ruzmaikin (1982) without a damping term[3] proportional to $1/T$

$$\frac{\partial \alpha_M}{\partial t} = \frac{\nu_t}{R^2}\frac{\partial^2 \alpha_M}{\partial x^2} - \frac{1}{\mu_0\rho}\left((\nabla\times\boldsymbol{B})\cdot\boldsymbol{B} - \frac{\alpha_0\cos x - \alpha_M}{\beta}|\boldsymbol{B}|^2\right), \tag{29}$$

where β is the combined (turbulent plus ohmic) diffusion of the field, ρ the density of the medium and μ_0 the magnetic constant.

Now using expression (2) for $\boldsymbol{B}$ and turning the system in a non-dimensional form using the same transformations as before, we obtain

$$\frac{\alpha_0\cos x - \alpha_M}{\beta}|\boldsymbol{B}|^2 = \frac{B_0^2\eta_t^2}{R^3\omega_0\beta}(D\cos x - C)\left(B^2 + \Gamma_1\left(\frac{\partial A}{\partial x}\right)^2\right), \tag{30}$$

where $\Gamma_1 = \frac{\eta_t^2}{R^4\omega_0^2}$ is a dimensionless constant. This allows the analogue of the Eq. (11) to be written in the form

$$\frac{\partial C}{\partial t} = \nu\frac{\partial^2 C}{\partial x^2} - \Gamma_2\times\left(\frac{\partial A}{\partial x}\frac{\partial B}{\partial x} - \frac{\partial^2 A}{\partial x^2}B\right) + \Gamma_3\times(D\cos x - C)\left(B^2 + \Gamma_1\left(\frac{\partial A}{\partial x}\right)^2\right), \tag{31}$$

where $\Gamma_2 = \frac{R^2B_0^2}{\eta_t^2\mu_0\rho}$ and $\Gamma_3 = \frac{R^2B_0^2}{\beta\eta_t\mu_0\rho}$ are dimensionless constants. Considering the same boundary conditions and spectral expansions as in the $\boldsymbol{J}\cdot\boldsymbol{B}$ case, Eq. (31) becomes

$$\begin{aligned}\frac{\partial C_n}{\partial t} = {} & -\nu n^2 C_n + \Gamma_2\left(\sum_{m=1}^{N}\sum_{l=1}^{N} H(n,m,l)A_m B_l\right) \\ & +\Gamma_3\sum_{m=1}^{N}\sum_{l=1}^{N} DB_m B_l H_1(n,m,l) \\ & +\Gamma_3\Gamma_1\sum_{m=1}^{N}\sum_{l=1}^{N} mlDA_m A_l H_2(n,m,l) \\ & -\Gamma_3\sum_{m=1}^{N}\sum_{l=1}^{N}\sum_{k=1}^{N} C_m B_l B_k H_3(n,m,l,k) \\ & -\Gamma_3\Gamma_1\sum_{m=1}^{N}\sum_{l=1}^{N}\sum_{k=1}^{N} lkC_m A_l A_k H_4(n,m,l,k),\end{aligned} \tag{32}$$

where H's are given by

$$\begin{aligned}H_1(n,m,l) = {} & \frac{1}{\pi}\left(\frac{m+1}{(m+1+l-n)(m+1-l+n)} - \frac{m+1}{(m+1+l+n)(m+1-l-n)}\right. \\ & \left. + \frac{m-1}{(m-1+l-n)(m-1-l+n)} - \frac{m-1}{(m-1+l+n)(m-1-l-n)}\right),\end{aligned} \tag{33}$$

$$\begin{aligned}H_2(n,m,l) = {} & \frac{1}{\pi}\left(\frac{n-l}{(n-l+m+1)(n-l-m-1)} + \frac{n-l}{(n-l+m-1)(n-l-m+1)}\right. \\ & \left. + \frac{n+l}{(n+l+m+1)(n+l-m-1)} + \frac{n+l}{(n+l+m-1)(n+l-m+1)}\right),\end{aligned} \tag{34}$$

$$\begin{aligned}H_3(n,m,l,k) = {} & \frac{1}{4}\left[\delta(m-l,k-n) - \delta(m-l,k+n)\right. \\ & \left. -\delta(m+l,k-n) + \delta(m+l,k+n)\right],\end{aligned} \tag{35}$$

$$\begin{aligned}H_4(n,m,l,k) = {} & \frac{1}{4}\left[\delta(m-n,l-k) + \delta(m-n,l+k)\right. \\ & \left. -\delta(m+n,l-k) - \delta(m+n,l+k)\right].\end{aligned} \tag{36}$$

Note that $\delta(n,m)$ is 1 if $n-m=0$ but 2 if $n=m=0$ and $H_1 = H_2 = 0$ if $n+m+l+1$ is even.

3.2.1. Results

Our results of the study of the system (15), (16) and (32) for positive dynamo numbers are depicted in Table 1. As can be seen, the effect of the inclusion of the $\alpha|\boldsymbol{B}|^2$ term is dramatic and seems to eliminate the possibility of chaotic behaviour for all N.

For the lower truncations of $N = 2$ and 3, we only observe fixed point solutions for all D up to $D \approx 2000$. For higher order truncations, with moderate D, there is a sequence of fixed points followed by stable periodic cycles.

The corresponding results for the negative dynamo numbers are shown in the Table 2, and again this is very similar to Table 1 with no evidence for chaotic behaviour at small and moderate D. In this case the $N = 2$ system has the origin as the fixed point for D down to -2000.

[3] The inclusion of this term will be studied in Sect. 4.

Table 1. Results for the case (II) for $D > 0$. D_1 indicates where the origin becomes unstable as a fixed point and D_2 the dynamo number where all fixed points become unstable and the solution becomes periodic

N	D_1	D_2
2	10	> 2000
3	15	> 2000
4	115	115
5	205	205
6	205	240
7	235	240
8	250	250

Table 2. Results for the case (II) for $D < 0$. D_1 indicates where the origin becomes unstable as a fixed point and D_2 the dynamo number where all fixed points become unstable and the solution becomes periodic

N	D_1	D_2
2	< -2000	< -2000
3	-70	-80
4	-85	-95
5	-85	-95
6	≈ -95	≈ -100
7	≈ -95	≈ -100
8	≈ -95	≈ -100

4. Case (III): robustness with respect to changes in the damping term

In this section we employ the equation proposed by Kleeorin et al. (1995) in the form

$$\frac{\partial \alpha_M}{\partial t} = -\frac{\alpha_M}{T} - \frac{1}{\mu_0 \rho}\left((\nabla \times \boldsymbol{B})\cdot \boldsymbol{B} - \frac{\alpha_0 \cos x - \alpha_M}{\beta}|\boldsymbol{B}|^2\right), \qquad (37)$$

as the evolutionary equation for the back reaction of the magnetic field on the time dependent part of α. In the above equation T is the characteristic time on which the small scale magnetic helicity changes, which is typically much longer than the turbulent diffusion time scale.

Using the same expression for $\boldsymbol{B}$ from Eq. (2) and proceeding in the same way as in the previous cases we obtain the differential equations for C_n to be

$$\begin{aligned}\frac{\partial C_n}{\partial t} = &-\Gamma_4 C_n + \Gamma_2\left(\sum_{m=1}^{N}\sum_{l=1}^{N} H(n,m,l) A_m B_l\right) \\ &+\Gamma_3 \sum_{m=1}^{N}\sum_{l=1}^{N} D B_m B_l H_1(n,m,l) \\ &+\Gamma_3\Gamma_1 \sum_{m=1}^{N}\sum_{l=1}^{N} ml D A_m A_l H_2(n,m,l) \\ &-\Gamma_3 \sum_{m=1}^{N}\sum_{l=1}^{N}\sum_{k=1}^{N} C_m B_l B_k H_3(n,m,l,k) \\ &-\Gamma_3\Gamma_1 \sum_{m=1}^{N}\sum_{l=1}^{N}\sum_{k=1}^{N} lk C_m A_l A_k H_4(n,m,l,k),\end{aligned} \qquad (38)$$

where $\Gamma_4 = \frac{R^2}{\eta_t T}$ is a dimensionless constant.

Table 3. Results for the case (III) for $D > 0$. D_1 indicates where the origin becomes unstable as a fixed point and D_2 the dynamo number where all fixed points become unstable and the solution is a periodic orbit

N	D_1	D_2
2	10	> 2000
3	15	> 2000
4	110	115
5	170	170
6	≈ 200	≈ 200
7	≈ 200	≈ 200
8	≈ 200	≈ 200

4.1. Results

Our results of the study of the system (15), (16) and (38) are shown in Tables 3 and 4. Although more modes are required in order to obtain convergence for higher dynamo numbers, the results shown in Table 3 and 4 seem to indicate that this type of change in the damping term does not produce qualitative changes in the behaviour of the system. This is reasonable, since the functional forms of the modal equations are quite similar in Eqs. (32) and (38).

The inclusion of the α_M/T term does not change the qualitative behaviour of the smaller truncations ($N = 2$ and 3 for $D > 0$ and $N = 2$ for $D < 0$, where we observe only fixed points as before). At moderate dynamo numbers, the qualitative behaviour is almost the same and remains periodic for $|D| > |D_2|$, but D_2 is changed slightly.

We also note that all systems considered here, in particular Cases (II) and (III), have a common pattern of behaviour, namely that as D is increased, A and B oscillate with slowly increasing amplitudes about zero. On the other hand, α_M oscillates with an increasing amplitude around a rapidly increasing average. Also if $D > 0$, α_M oscillates about a positive average and about a negative average for $D < 0$.

5. Conclusions

We have studied the robustness of truncated $\alpha\Omega$ dynamos including a dynamic α equation, with respect to physically motivated changes in the driving term and a change in the damping

Table 4. Results for the case (III) for $D < 0$. D_1 indicates where the origin becomes unstable as a fixed point and D_2 the dynamo number where all fixed points become unstable and the solution is a periodic orbit

N	D_1	D_2
2	< 2000	< 2000
3	-70	-80
4	-80	-95
5	-95	-95
6	≈ -95	≈ -105
7	≈ -95	≈ -110
8	≈ -95	≈ -110

term appearing in the dynamical α equation. We studied these systems with respect to changes in the dynamo number D, the truncation order N and the IC. Our results show that the changes in the driving term have important effects on the dynamical behaviour of the resulting systems. In particular we find that

– chaos is much less likely in systems with a driving term of the form $\boldsymbol{J} \cdot \boldsymbol{B}$ (with positive D), as opposed to those involving $A_\phi B_\phi$.
– the inclusion of the $\alpha|\boldsymbol{B}|^2$ term has a dramatic effect in that it suppresses the possibility of chaotic behaviour at moderate dynamo numbers.
– changes in the sign of the dynamo number can also produce important changes. In the case where the driving term is given by $A_\phi B_\phi$, using $D < 0$ makes chaotic behaviour much less likely (which seems to be the mirror image of the case where the driving term given by $\boldsymbol{J} \cdot \boldsymbol{B}$ and $D > 0$).
– in case (I) there exists substantial intervals of D for which the systems seem to possess ”multiple attractors” (consisting of equilibrium and periodic states). As a result small changes in either D or the IC can produce important changes in these regimes. This form of fragility can be of importance, especially in presence of noise, where the system would behave in an intermittent way.

Finally to recapitulate our motivation for studying different formulations of dynamic α feedback, we note that even the usual expression for the driving term, $\boldsymbol{J} \cdot \boldsymbol{B}$, derived from first principles could still be inappropriate, as it involves uncontrolled approximations. However, it is clear that f has to be a pseudo-scalar (because α is a pseudo-scalar), and the most obvious possibilities are indeed the ones that we have studied. Our investigations have shown that the actual choice can significantly alter the overall conclusion. Therefore, all conclusions, especially those concerning the occurrence of chaos, should be taken with utmost care.

Acknowledgements. EC is supported by grant BD / 5708 / 95 – Program PRAXIS XXI, from JNICT – Portugal. RT benefited from SERC UK Grant No. H09454. This research also benefited from the EC Human Capital and Mobility (Networks) grant “Late type stars: activity, magnetism, turbulence” No. ERBCHRXCT940483.

References

Brandenburg, A., Krause, F., Meinel, R., Moss, D., Tuominen, I., 1989a, A&A, **213**, 411
Brandenburg, A., Moss, D., Tuominen, I., 1989b, Geophys. Astrophys. Fluid Dyn., **40**, 129
Brandenburg, A., Moss, D., Rüdiger, G., Tuominen, I., 1990, Solar Physics, **128**, 243
Brandenburg, A., Nordlund, A., Stein, R.F., Torkelsson, 1995, ApJ, **446**, 741
Choudhuri, A., 1990, ApJ, **355**, 733
Coley, A.A., Tavakol, R.K., 1992, Gen. Rel. Grav., **24**, 835
Feudel, F., Jansen, W., Kurths, J., 1993, Int. J. Bifurc. Chaos, **3**, 131
Gilman, P.A., 1983, ApJS, **53**, 243
Kleeorin, N. I., Ruzmaikin, A.A, 1982, Magnetohydrodynamica,**N2**, 17
Kleeorin, N. I, Rogachevskii, I., Ruzmaikin, A., 1995, A&A, **297**, 159
Krause, F., Rädler, K.-H., 1980, *Mean-Field Magnetohydrodynamics and Dynamo Theory*, Pergamon, Oxford
Lorenz, E. N., 1963, J. Atmos. Sci., **20**, 130
Newhouse, S., Ruelle, D., Takens, F., 1978, Comm. Math. Phys.,**64**, 35
Ruelle, D., Takens, F., 1971, Comm. Math. Phys., **20**, 167; **23**, 343
Schmalz, S., Stix, M., 1991, A&A, **245**, 654
Smale, S. 1966, Amer. J. Math., **88**, 491
Sparrow, C., 1982, *The Lorenz Equations*, Springer-Verlag, New York
Tavakol, R.K., Ellis, G.F.R.,1988, Phys. Lett., **130A**, 217
Tavakol, R.K, Tworkowski, A. S., Brandenburg, A., Moss, D., Tuominen, I., 1995, A&A, **296**, 269
Tobias, S.M., Weiss, N.O., Kirk, V., 1995, MNRAS, **273**, 1150
Weiss, N. O., Cattaneo, F., Jones, C. A., 1984, Geophys. Astrophys. Fluid Dyn., **30**, 305
Zeldovich, Ya.B., Ruzmaikin, A.A, Sokoloff, D.D, 1983, *Magnetic Fields in Astrophysics*, Gordon and Breach, New York

This article was processed by the author using Springer-Verlag LaTeX A&A style file *L-AA* version 3.